

# The derepression of transposable elements in lung cells is associated with the inflammatory response and gene activation in idiopathic pulmonary fibrosis

Mahboubeh R Rostami

Weill Cornell Medical College: Weill Cornell Medicine

Martina Bradic (✉ [bradicm@mskcc.org](mailto:bradicm@mskcc.org))

NewYork-Presbyterian Hospital/Weill Cornell Medical Center <https://orcid.org/0000-0001-6078-5311>

---

## Research

**Keywords:** idiopathic pulmonary fibrosis, IPF

**Posted Date:** January 27th, 2021

**DOI:** <https://doi.org/10.21203/rs.3.rs-80034/v2>

**License:**  This work is licensed under a Creative Commons Attribution 4.0 International License.

[Read Full License](#)

---

# Abstract

## Background

Transposable elements (TEs) are repetitive sequences of viral origin that compose almost half of the human genome. These elements are tightly controlled within cells, and if activated, they can cause changes in both gene regulation and immune viral responses that have been associated with several chronic inflammatory diseases in humans. As oxidants are potent activators of TEs, and because oxidative injury is a major risk factor in relation to idiopathic pulmonary fibrosis (IPF), we hypothesized that TEs might be involved in the regulation of gene expression and so contribute to inflammation in cases of IPF. IPF is a fatal lung disease that involves the gradual replacement of the alveolar tissue with fibrotic scars as well as the accumulation of inflammatory cells in the lower respiratory tract. Although IPF is known to occur as a result of the complex interaction between age, environmental risk factors (i.e., oxidative stress) and genetics, the relative contributions of these factors to the disease remain unclear. To determine whether TEs are associated with IPF, we compared the transcriptional profiles of the genes and TEs of lung cells obtained from both healthy donors and IPF patients.

## Results

We quantified the TEs and gene expression levels using a published bulk RNA-seq dataset concerning 24 subjects (16 donors and eight IPF patients), including three lung-cell types per subject, as well as a scRNA-seq dataset concerning 16 subjects (eight donors and eight IPF patients).

We found evidence of TE dysregulation in the alveolar type II lung cells and alveolar macrophages of the IPF patients. In addition, the activation of the LINE1 family of elements in IPF is associated with the increased expression of TE cellular regulators (MOV10, IFI16, SAMHD1, and APOBECG3), interferon-stimulating genes (ISG15, IFI6, IFI27, IFI44, and OAS1), chemokines (CX3CL1 and CXCL9), and interleukins (IL15RA). We also propose that TE derepression might be involved in the regulation of previously reported IPF candidate genes (MUC5B, CHL1, SPP1, and MMP7).

## Conclusion

Based on our findings, we propose that TEs derepression play an important role in the regulation of gene expression and can also prompt both the recruitment of inflammatory processes and the disruption of the immunological balance, which can lead to chronic inflammation in IPF.

## Background

Over half the human genome is composed of repetitive sequences known as transposable elements (TEs). These repeated regions of the genome are organized into DNA transposons, which propagate via a cut and paste mechanism, and retrotransposons, which move by means of a copy and paste mechanism [1, 2]. Retrotransposons are the most prevalent TEs in humans, and they are further divided

into the long terminal repeats (LTR) superfamily, which includes endogenous retroviruses (ERV), and the non-LTR superfamily, which includes both short interspersed elements (SINEs) and long interspersed elements (LINEs). Each of these superfamilies harbors a diverse family of repetitive sequences, and only the non-LTR elements from the L1, *Alu*, and SVA families can still transpose in the human genome [3]. TE transposition can destabilize the genome in many different ways, including gene disruption, the modulation of gene transcription, and mRNA processing through numerous mechanisms [4, 5]. Given their viral origin, the overexpression of TEs can also mimic viral infection and so trigger an innate immune response, leading to chronic inflammation [6, 7]. Although the TE activity is tightly regulated in somatic cells at the transcriptional and post-transcriptional levels, dysregulation can occur due to changes in DNA methylation, histone modification, or mutations in the genes involved in TE regulation [8-10]. Notably, elevated cytokine levels and chronic inflammation in response to increased TE expression have previously been demonstrated in relation to various human diseases, including multiple sclerosis, systemic lupus, lateral sclerosis, Rett syndrome, Aicardi-Goutières syndrome, aging-related pathologies and complex lung disorders [11, 12]. However, due to their repetitive nature, TEs are often excluded from analysis, which explains why their effect on expression and their involvement in the processes of diseases have not been systematically studied. Here, we aim to survey the TE activity in idiopathic pulmonary fibrosis (IPF) as well as to determine whether TE activation might be involved in both the IPF-related inflammatory response and the regulation of IPF-related genes.

IPF is a non-treatable inflammatory lung disease that involves the gradual replacement of the alveolar tissue with fibrotic scars as well as the accumulation of inflammatory cells in the lower respiratory tract [13]. The detection of IPF-associated genetic variants has enhanced our understanding of the role played by inherited risk factors in the disease risk. However, the underlying causes of IPF are not yet well understood, while vital questions persist regarding the ways in which the complex interaction between risk factors (e.g., smoking, viral infection, oxidative stress, age) and genetics causes the pathogenesis of IPF [14]. An important feature of that pathogenesis is the shift in epithelial cell populations whereby type I alveolar (AT1) epithelial cells are damaged and the epithelial surface is populated by type II alveolar (AT2) epithelial cells and bronchiolar epithelial cells. The lower respiratory tract of an IPF patient is primarily populated by alveolar macrophages (AMs) and neutrophils, which are among the first responders to cellular defense and which play a significant role in absorbing harmful particles that have passed through the mechanical barrier of the respiratory system. When activated, AMs spontaneously release toxic oxidants (i.e.,  $H_2O_2$ ), which place a persistent oxidative burden on the fragile structure of the alveoli, and therefore, represent one of the most important mechanisms of AT2 epithelial cell injury in cases of IPF [15, 16].

As oxidants are potent activators of TEs [17], we hypothesized that exposure to oxidative stress fosters a permissive environment in lung cells that unleashes TEs, which modify the adjacent gene expression and also contribute to chronic inflammation due to their “viral mimicry” potential. To test this hypothesis, we used published transcriptome profiles of lung cells obtained from both healthy donors and pulmonary fibrosis patients [18]. This data were chosen because it allows for the profiling of the TE activity in the

individual cell populations within those cells that are highly relevant to the disease. We determined the upregulation of TEs in IPF patients using the bulk RNA sequencing data in AT2, AM, and whole-lung cells, and we confirmed the upregulated TE activity of the L1 TE family in individual cell clusters using single-cell RNA sequencing (scRNA-seq) data. This is the first study to survey and relate TE activity to IPF. Additionally, it demonstrates that TE derepression might be involved in the regulation of the previously reported IPF candidate genes, and further, that active TEs might be involved in the perpetual inflammation of the lower respiratory tract in cases of IPF.

## Results

### Increased TE expression is positively correlated with both the activation of cellular TE inhibitors and the innate immune response and negatively correlated with autophagy in IPF

To determine the expression of TEs changes in IPF, we quantified the TE expression from previously published reports of the bulk RNA sequencing of 14 donor lung biopsies and compared it to explants from eight transplant recipients [18] (**Supplemental Table 1**). We first compared the gene expression and expression of the TE families between IPF patients and donors in flow cytometry-sorted AMs, AT2 cells, and whole lungs (WLs). The TE families are defined as groups of TEs with similar sequences across the genome (subfamilies), and thus, their expression is averaged per the number of such groups.

The largest changes in the expression of the TE family were identified in the AT2 cells (72 up, 22 down), with the largest number of changes being present in the LTR-TEs (**Figure 1, Table 1A, Supplemental Table 2 A-C**). The WL that represents a mixture of different cell types exhibited 18 TE subfamily differences (14 up, 4 down), with the largest number of changes again being present in the LTR-TEs. Finally, the TE activity in the AMs was characterized by 17 TE subfamily differences (11 up, 6 down), again primarily in the LTRs. A few other TE expression changes representing DNA transposons, which are less abundant TE families in humans, were also identified. The changes in the gene expression showed the same trend as the TE changes, and they were also the highest in the AT2 cells (4131), followed by the WL (1170) and AMs (1033) (**Table 1A**). We performed a Fisher exact test [19] to assess whether differentially expressed subfamilies are enriched in WL, AT2, or AM cells, and we did not find any significant enrichment (**Table 1B**). Interestingly, the LINE elements, which are responsible for the majority of retrotransposition activity in humans, were only upregulated in the AT2 cells (**Figure 1, Table 1A**). To confirm our findings, we also analyzed the data using *REdiscoverTE* [20] and verified the largest number of TE changes in the AT2 cells with similar changes in the individual subfamilies (**Supplemental Figure 1, Supplemental Table 2 D-G**).

AT2 cells are a primary target of injury in IPF, and the processes involved in AT2 cellular senescence and inflammation are crucial for the development of fibrotic lung disease [21-25]. Moreover, the LINE TE family, particularly the upregulation of the autonomous (expressed from intergenic region, i.e., not from genic region and thus not dependent on gene expression) L1HS subfamily, has a well-established impact on senescence-related inflammation [6, 7]. Thus, we first tested for any evidence of autonomous L1HS

subfamily upregulation in the AT2 cells. To differentiate autonomous TE expression from co-expression with host genes or intron retention, we used *REdiscoverTE* [20]. This computational workflow is designed to separate reads at the family level according to their genomic location (intronic, exonic, and intergenic), and it specifically models autonomous TE expression. We observed the largest number of differentially expressed TE families in the IPF cells in the exonic region (65), followed by those in the intergenic (57) and intronic (32) regions (**Supplemental Table 3A-D**) if only the SINE, LINE, and LTR families were considered. Differential expression in the intergenic region (autonomous TE expression) is however only relevant change for determining TE impact on cellular processes [20, 26]. We detected overexpression of 16 LINE subfamilies, 38 LTR families, and three SINE families in the intergenic regions of the IPF cells (**Supplemental Table 3C**). These were all evolutionary old TEs [27]; they were excluded from this particular analysis because their relationship with the inflammation during cellular senescence is functionally not well-established. Importantly, the L1HS family that represents human specific and retrotransposition competent TE element was significantly upregulated only in the intergenic region of the IPF cells (**Figure 2A, Supplemental Table 3C**) [28]. This suggests autonomous L1HS expression that could be related to the cellular processes involved in IPF. A similar pattern of differential intergenic TE expression in AT2 was observed using the modified *SQUIRE* quantification method (see Materials and Methods for details) (**Supplemental Table 3D and Table 3E**). The L1HS expression between groups as quantified by the modified *SQUIRE* quantification method was significantly different ( $p=0.037$ ,  $\log_{2}FC=1.16$ ) as per *DESeq2* analysis prior to multiple test correction ( $p=0.11$ ). (**Supplemental Figure 2**). This discrepancy is a result of different mapping and quantification methods used by *SQUIRE* and *REdiscoverTE*.

AM and WL cells were also inspected for L1HS intergenic expression, and no differential expression was detected between the IPF and donor cells (data not shown).

TEs are tightly controlled by multiple mechanisms, including TE promoter methylation, and the inhibitory host factors involved in transcriptional and post-transcriptional TE control [29]. Modifications in these control points might activate TEs and cause pathological states that are frequently accompanied by inflammation [6, 11, 20, 30]. However, cellular transformation to a disease state in IPF is also complemented by these processes [21, 22, 31]. Thus, we determined whether there was an association between L1HS upregulation, and the expression of genes with functional relevance to L1HS activity [29, 32]. We tested four gene sets from the published literature: type I interferons (IFN-I, 84 genes), senescence-associated secretory phenotype (SASP) genes (85 genes), L1 transcriptional regulator genes (two genes), and L1 post-transcriptional regulator genes (17 genes) using linear model.

A total of 73 of these genes were differentially expressed between the IPF and donor cells; 63 were upregulated and ten were downregulated out of the 188 genes from our four sets (**Supplemental Table 4B-C**). Our linear model analysis showed a significant association between L1HS and 60 genes that differed between the IPF and donor cells (**Supplemental Table 4C**).

Here, we highlighted a correlation between L1HS and a few well known functionally important genes. We observed a positive association between L1HS and the forkhead box A1 (FOXA1) transcription factor (TF), which is crucial for L1HS expression; this finding is further evidence of the active expression of L1HS in the IPF cells (**Figure 2C, Supplemental Table 4C**) [6]. However, post-transcriptional regulator CALCOCO2 (NDP52), which plays an important role in degrading L1 RNA in the cytoplasm [33], was downregulated in the IPF patients and negatively correlated with the expression of L1HS (**Figure 2C, Supplemental Table 4C**). This might suggest an uncontrolled accumulation of L1HS in the IPF cells. Genes involved in IFN-I response (e.g., DDX58 (RIG-I), IFI16, STAT1, IRF9, ISG15), which is important for recognition of L1 cytosolic accumulation, and downstream activation of inflammatory processes also showed positive correlations with L1HS [29] (**Figure 2C, Supplemental Table 4C**). This further suggests that the inflammatory processes in IPF cells are related to increased L1HS expression.

We also tested genes that act as L1HS post-transcriptional regulator genes and found positive correlations for *three of them in the IPF cells* (**Figure 2C [SAMHD1, MOV10, APOBEC3G], Supplemental Table 4-C**). [29]. Some of these L1 inhibitors, such as SAMHD1, MOV10, and APOBEC3G, are activated by IFNs [34]. Thus, increased interferon signaling may have activated these L1 inhibitors against the high L1HS expression in the AT2 cells.

Finally, SASP markers (e.g., SERPINE1 and MMP3) were also positively associated with L1HS in the IPF cells [6] (**Figure 2C, Supplemental Table 4-C**). This is particularly interesting, as previous research showed increased SERPINE1 in IPF AT2 senescent cells [35]. Increased MMP3 expression is also essential for the pathogenesis of IPF, based on findings from IPF patients and animal models [36]. We found extremely low MMP3 expression in the donor cells, whereas the IPF cells expressed high levels of MMP3, which was positively associated with L1HS. This further suggests that senescent cells in IPF patients also exhibit an increase in L1HS activity.

### **Locus-level TE expression is associated with IPF and is also cell-type specific**

The induction of immune response in cellular senescence by means of the accumulation of the intrinsically expressed TEs in the cell is not the only detrimental effect of TEs. Indeed, TEs can provide alternative promoters or polyadenylation signals, as well as alternative splice acceptor and donor sites, which can strongly alter the gene expression patterns of the host. [5, 37]. In addition, a few methods based on the association between TE and –proximal gene expression have been developed as potential tools for detecting candidate genes for diseases [38].

Here, we aim to determine whether locus-specific TE expression near or within the gene can explain the expression differences of that gene, and whether that relationship differs between donor and IPF cells. We quantified the changes in TE expression that occurred at individual genomic locations for all TE families within the three cell types, and associated those differences with adjacent gene expression. We again identified the largest number of changes in the AT2 cells (1489 up, 1149 down), while the WL also featured an abundant number of changes representing 1341 TE loci (588 up, 753 down) (**Figure 3, Supplemental Table 5**). Finally, the TE activity in the AM was found to be characterized by 359 TE loci

(193 up, 166 down). We first intersected the upregulated TE locus changes as well as the gene changes between the IPF patients and the healthy donors in each cell type (**Figure 4A**). This analysis revealed that most changes were unique and only present in an individual cell type (AT2 = 1426, AM = 180, and WT = 530), although 53 TE changes were shared between the AT2 and WL, four between the WL and AM, and nine between the AM and AT2, while one change was common to all three comparisons. This suggests the potentially strong impact of TE activity specific to the AT2 and AM that might affect the gene expression related to IPF and that is not detected when analyzing the heterogeneous WL cell population. The number of gene expression changes shared among the different cell types also showed a similar trend, with the highest number of expressed genes being observed in the AT2 (3826), followed by the AM (822), and the WT (644).

We next examined the distribution of the TE changes across the genomic regions. To do so, all the differentially expressed TE changes were categorized as belonging to either the 5'UTR, 3'UTR, exon, intron, or intergenic region. These analyses revealed the same pattern of changes as observed in relation to the three comparisons (**AT2, AM, and WL, Figure 4B, Supplemental Table 5**), with the highest number of TE transcriptional changes being seen in the 3'UTR region, while the smallest number of changes were found in the intron and intergenic regions. The TE changes overlap with the exon as well as the exon-intron, exon-5'UTR, and exon-3'UTR regions were excluded from further analysis because they were most likely related to transcriptional noise.

### **TE expression is correlated with the gene expression of several IPF candidate genes**

To further illustrate the importance of locus-specific TEs, we tested the effects of the intragenic and intergenic upregulated TE (excluding those in the exons) loci on the transcriptional regulation of the genes. As the pairwise comparisons of each gene with each TE locus identified a large number of changes, some of which proved difficult to interpret, we focused on the TEs matched with their adjacent genes (cis interactions) and examined whether TE expression predicts nearby gene expression. There were 1512 pairs (out of 10092988 tests conducted between 3826 genes and 2638 TEs, with 7.80% being significant pairs) in the AT2 cells, 198 pairs in the AM cells (out of 295098 tests conducted between 822 genes and 359 TEs, with 1.4% being significant pairs), and 497 pairs in the WL (out of 863604 tests conducted between 644 genes and 1341 TEs, with 0.04% being significant pairs) that matched the cis criteria (**Figure 5**). We identified a total of 172, 105, and four significant gene-TE pairs ( $p < 0.05$ ) from among our cis subsets in the AT2, AM2, and WL, respectively. In some cases, there were more than one TE associated with the expression of the same gene. Thus, we further classified the difference into the number of unique genes whose transcription is significantly related to the TEs. This classification resulted in the identification of a total of 107 genes in the AT2 cells, 63 genes in the AM cells, and three genes in the WL tissue that had a transcriptional pattern correlated with TEs and that differed between the IPF patients and the healthy donor (**Figure 5**). Interestingly, although a high number of TE-gene pairs were present in the WL comparison, only a very few significant differences were observed, which again

suggests that important signatures might be missed in heterogeneous cell populations. Our gene ontology enrichment analysis of the genes found to be correlated with TE expression in the AT2 cells identified cilium movement as well as axoneme and organelle assembly related processes (FDR < 0.005) (**Table 2A**). This suggests that the activation of TEs can result in the activation of genes that might be involved in cellular identity changes. In the AM cells, the TE-associated gene expression was found to be linked with immune-related cellular process.

Most of the TEs found to be associated with gene regulation in the AT2 cells were identified in the introns (75), followed by the 3'UTR region (82), outside the gene (12), and the 5'UTR region (three) (**Supplemental Table 6A, Table 2B**). The SINE (Alu) elements were most commonly found to be associated with gene expression in the AT2 cells, and they were mostly embedded within the 3'UTR region of the genes. Several of the genes found to be significantly correlated with TEs represent important IPF candidate genes that have been identified in multiple genome-wide association studies or functional studies related to IPF [39]. For example, we identified a 3.88-fold expression change between the IPF patients and the healthy donors in the TE (chr11|1253519|1253937|MLT1C:ERVL-MaLR:LTR) that is located between exons 33 and 34 and that is significantly correlated with the high expression of the MUC5B gene in IPF (**Supplemental Table 6A**). Furthermore, the relationship between the gene and the TE expression of IPF group is significantly different than the same relationship in donor group (Figure 6A, p.adjust=0.0284). This suggests the potential role played by TEs in the regulation of this gene, which in turn plays an important role in mucin excretion and significantly contributes to IPF pathogenesis [40, 41]. Notably, we identified the association between one of the three core IPF gene markers, namely the cell adhesion molecule L1-like (CHL1) gene, and the L1PA6 TE (chr3|367661|374053|L1PA6:L1:LINE) (**Supplemental Table 6A**). However, two other TEs (chr3|391232|391535|AluSz:Alu:SINE, chr3|408347|408547|MIRc:MIR:SINE|342), also showed a significant association with CHL1 expression. To determine which of the TEs made the largest contribution to CHL1 gene expression, we used all three TEs in a linear model and then calculated the relative importance of each of them in terms of influencing CHL1 expression. The proportion of the variance explained by the model containing all three TEs was 86.09%. Further, each TE explained ~20% of the variance, while the group covariate representing the phenotype explained ~25% of the variance, thereby suggesting the similar contributions of all the TEs to the gene expression. Significant difference between the correlation slope in IPF and donor groups was also observed for L1PA6- CHL1 relationship (Figure 6A, p.adjust= 0.0019) and the other two TEs (AluSz, MIRc) associated with CHL1. This further suggests potential regulation of CHL1 by adjacent TEs in IPFs.

*The serpin family B member 3 (SERPINB3) is another important IPF candidate gene for which we identified a 4.23-fold change in the gene expression between the IPF patients and the healthy donors, which was correlated with a 4.21-fold change in the LINE TE element (chr18|63651629|63653187|L1MA8:L1:LINE) (Supplemental Table 6A). This element is located ~2 kb downstream of the gene. Glutathione S-transferase alpha 2 (GSTA2) also exhibited upregulation in the*

IPF patients, and its expression was associated with the LTR5A TE (chr6|52748278|52749305|LTR5A:ERVK:LTR) located 783 bp downstream of that gene (*Figure 6A, Supplemental Table 6A*). Although TEs significantly predicts the expression of *SERPINB3* and *GSTA2* genes, that relationship does not significantly differ between IPF and donors as shown by test for correlation slopes (*Figure 6A*,  $p_{\text{adjust}}=0.1260$ ,  $p_{\text{adjust}}=0.9227$ , respectively). Nevertheless, significant difference of TEs expression results in significant difference in gene expression for these genes in IPF suggesting their role in the disease.

The analysis of the TE loci in the AM cells primarily determined the association between gene expression and the SINE elements (56), followed by the LINE (26), LTR (six), and 17 other elements (e.g., DNA transposons) (**Supplemental Table 6B, Table 2B**). Most of the elements from all the families were activated within the 3'UTR region, and we did not identify any elements associated with gene expression outside the gene. We found that the expression of the chemokine *CCL22* was related to the three SINE elements (chr16|57364478|57364778|AluSq2:Alu:SINE, chr16|57364806|57365101|AluSz:Alu:SINE, chr16|57365617|57365740|AluJo:Alu:SINE) located in the 5'UTR and 3'UTR region (**Table 4B**). This chemokine contributes to activation of alveolar macrophages and subsequently to the lung damage in patients with IPF [42]. The proportion of variance explained by the model predicting the *CCL22* expression was 93.71%, with AluSz (3'UTR) explaining ~29% and AluJo (3'UTR) and AluSq2 (5'UTR) explaining ~27% and ~24%, respectively. Correlation slopes for IPF and donors are also significantly different for two of these elements providing additional evidences for strong regulation of *CCL2* by TEs activation in IPF patients (*Figure 6B, only plot for AluSq2 element is shown*,  $p_{\text{adjust}}= 0.0237$ ). We also found that the upregulated TE expression in the intron (chr14|22843913|22844208|AluSx1:Alu:SINE), and in the 3'UTR region (chr11|102520549|102520704|L2c:L2:LINE) significantly correlates with two upregulated matrix metalloproteases (*MMP14* and *MMP7*, respectively) in IPF group (**Supplemental Table 6B**). MMPs are important players in cell migration and tissue repair in lungs and have been related to IPF pathogenesis [43]. Here, we establish correlation of two MMPs with TEs and we further identify significant TE-gene correlation slope difference in *MMP7* between IPF and donors which further confirms differential regulation of *MMP7* in IPF (*Figure 6B*,  $p_{\text{adjust}}= 0.0156$ ).

We were also able to associate a number of other genes with TE expression that have previously been related to IPF, including osteopontin (*SPP1*) in the 3'UTR region (Chr4: 87979662-87979893)

and the interleukin 1 receptor antagonist (*IL1RN*) within the 5'UTR region (chr2|113133292|113133561|Charlie18a:hAT-Charlie:DNA) (**Supplemental Table 6B**). Both these genes are known to be expressed at high levels in IPF AM cells, while previously reported immunohistochemistry results have confirmed that these markers are not expressed in donor tissue [18]. Our study also finds significant upregulation of these genes and their adjacent TE loci in IPF.

However regression slopes between donors and IPF did not differ for these two TE-gene pairs, suggesting that these genes might not be directly related to TE expression (*Figure 6B*,  $p_{\text{adjust}}= 0.1739$  for *SPP1*,  $p_{\text{adjust}}= 0.8381$  for *IL1RN*).

### ScRNA-seq analysis confirms the TE changes in multiple cell populations in the fibrotic human lung

We also analyzed a previously published dataset concerning eight donors and eight IPF patients that had been generated by means of scRNA-seq technology [44]. A total of 77,517 single cells and 22,009 genes were obtained. We assigned each cluster to a cell type based on the expression of the established markers in that cluster (**Supplemental Figure 3**), and the following cell types were confirmed: epithelial cells (alveolar type II cells (AT2), alveolar type I cells (AT1), ciliated cells, basal cells, and club cells), immune cells (alveolar macrophages (AMs), monocytes, B cells, plasma mast cells, dendritic cells, and T cells), and mesenchymal cells (fibroblasts and endothelial cells) (**Figure 7A**). The distribution and identity of the cells were similar between the two phenotypes (**Figure 7B, Supplemental Table 5A**). To confirm the differential TE activity in the AM2 and AT2 cells in the IPF patients, as well as to determine whether the TEs differed in the other cell types, we performed a differential gene expression (DGEs) analysis between the donors and the IPF patients with regard to the TE subfamilies in each cell type (**Supplemental Table 7B**). The results of the DGEs analysis between the IPF patients and the donors for each identified TE subfamily and all the genes in the individual lung cell type are presented in **Supplemental Table 7C** and summarized in **Figure 7C**. We identified the increased transcription of two TE families (LINE and LTR) in the IPF patients when compared with the donors in multiple cell types ( $p_{\text{adjust}} < 0.05$  and  $\text{log}_2 \text{FC} > 0$ ). Consistent with the TE upregulation identified in our RNA bulk analysis, we identified 27 significantly upregulated L1 subfamilies and eight significantly upregulated LTR subfamilies in the single-cell transcriptome. Similarly, 22 LINE subfamilies and 12 LTR subfamilies were found to be upregulated in the AM cells (**Figure 7C**). In addition, we also detected upregulation in the case of the IPF patients in the monocytes as well as the upregulation of a smaller number of subfamilies in the club, ciliated, B, dendritic, AT1, T, endothelial, and plasma cells.

Aside from identifying changes in multiple subfamilies, we were also interested in determining whether an association exists between the total expression of the L1 subfamilies and IPF in AT2 cells, as identified by bulk RNA-seq. Thus, we calculated the L1 score that represents the average expression of the upregulated L1 family per each cell type. The comparison between the L1 scores of the healthy donors and the IPF patients indicated that the L1 score is significantly higher among fibrosis patients in the AT2 cells, which indicates that it might be involved in IPF pathogenesis (**Figure 8A**). To further confirm whether the relationship between L1 activity (L1 score) and TE-related genes differs

among the IPF patients and the healthy donors, we tested 126 genes which were identified in bulk RNA-seq. We identified 27 TE regulation and inflammatory response related genes ( $p_{\text{adjust}} < 0.05$ ) (i.e.

APOBE3G, STAT1, SAMHD1, IRF9) in the AT2 cells (**Supplemental Table 7D, Figure 8B**). This observation indicates that the L1 upregulation, also confirmed in independent dataset by scRNA-seq might promote the inflammatory response in the AT2 cells of IPF patients. Single-cell RNA sequencing is a powerful method but only generates short reads from one end of a cDNA template, limiting the mapping of highly similar TE sequences. Thus, locus specific TE expression was not performed for scRNA seq dataset.

## Discussion

### TEs and inflammation in IPF

The derepression of TEs can cause changes at the transcriptional and post-translational levels that involve gene expression changes, and further, that recruit immune signaling pathways that might result in pathologies [5, 45-47]. Our study suggests potential involvement of TEs in IPF, and we find evidence that TEs are significantly upregulated in the AT2 cells of fibrotic lungs. Aside from the overexpression of TEs in AT2 IPF cells, we also find that the dysregulation of TEs is likely further facilitated by the decreased expression of the autophagy gene CALCOCO2 (NDP52), which is known to be crucial receptors for the detection and removal of at least one TE RNA family (L1). Dysfunctional autophagy has also been previously associated with IPF, with the suggestion being that it promotes the epithelial–mesenchymal transition of the AT2 cells contributing to fibrosis [48]. Moreover, the failure of the autophagosome removal of TEs leads to cytoplasmic TE accumulation, which can result in genome instability and inflammation [33] and, in turn, can contribute to IPF.

Pulmonary fibrosis is known to be accompanied by innate and adaptive immune responses; however, the role of inflammation in the disease remains unclear [31]. We propose that L1HS activation and accumulation in AT2 cells might represent an important trigger of the viral cellular sensors and the activation of the innate immune system (macrophages), thereby resulting in the disruption of the immunological balance, which can cause chronic inflammation in IPF. Many of the inflammation-related processes that we associate with TEs have also been previously described as contributing to IPF (IFI6, IFI27, IFI44, OAS1, IL15RA, CX3CL1, and CXCL9) (**Supplemental Table 4-C**), and they are known to be involved in both fibroblast activation and the accumulation of the extracellular matrix [49]. Furthermore, we confirm some of these processes in our single-cell data analysis, which also shows the highest TE LINE upregulation in the AT2 cells as well as its correlation with some of the genes related to the inflammatory response in IPF patients (i.e. IRF9, STAT1).

The age-related onset of IPF is further evidence that TEs might be involved in IPF and linked to the inflammatory response. Indeed, IPF is most prevalent in individuals aged 60 years or older, and it is partially mediated by senescent cells [21, 50]. The upregulation of intergenic L1HS that positively correlates with SASP markers (i.e., MMP3 and SERPINE1) in AT2 cells suggest that cellular senescence in

IPF might be important for L1HS activation. One of the major triggers of cellular-senescence-associated inflammation is the activation of L1 TEs by the age-related loss of epigenetic marks [6, 51]. In accordance with these findings, our study shows the significant upregulation of FOXA1 TF that can bind to the demethylated L1 promoter and thus induce L1HS expression (**Figure 2B-C, Supplemental Table 4B-C**). This could potentially result in the activation of the cytosolic sensors for ssDNA (i.e., IFI16), which are responsible for signaling through the cGAS–cGAMP–STING pathway and could induce both interferon-related changes and age-associated inflammation [6, 7]. Indeed, numerous INF- $\gamma$  related genes were upregulated and associated with L1HS expression in IPF cells (**Supplemental Table 4B-C**). This supports the previously reported importance of cellular senescence, and inflammation in IPF AT2 cells and their potential interaction with L1HS upregulation [25, 52]. We expect future work to uncover additional mechanisms involved in TE activation in IPF.

### **Expression of TE loci is associated with expression of IPF related genes**

The inflammatory response is not the only outcome of uncontrolled global TE expression, as the activity of individual TE loci can also play an important role in modulating the expression of adjacent genes [47]. Our data show that the TE expression in the vicinity of several genes is associated with the gene expression in both the AT2 and AM cells in the IPF patients. Notably, some of these genes have previously been associated with IPF. For example, the MUC5B promoter variant is one of the major IPF risk factors associated with an increase in gel-forming mucin, which produces mucosal host defensive dysfunction in the bronchi and so is critical in IPF [53]. Our observation that TEs might be involved in the regulation of this gene is based on the significantly higher expression in IPF patients noted from TEs embedded in the intronic region of the gene. Other examples relevant to TEs include the CHL1 gene, which *exhibits* > 0.8 specificity and 0.9 sensitivity in distinguishing IPF patients from healthy controls, meaning that it is a potential IPF drug target [54]. Although no studies have yet related the TEs in CHL1 with IPF, previous studies have *proposed that the L1P6 TE within CHL1 can act as an L1 antisense promoter and so drive the transcription of chimeric transcripts* [55]. *Our study also shows the upregulation of L1P6 to explain ~25% of the CHL1 expression, which indicates that this gene might potentially play a regulatory role in relation to CHL1 and so contribute to IPF. One of the fundamental genes* associated with the control of proteolysis (SERPINB3) [32], together with the GSTA2 gene, which has previously been associated with IPF [56], show potential regulation from TEs outside the gene. Both these genes have TEs located in close downstream proximity (within 2 kb) to the gene, and while they were not formerly described in other studies, they might have an AT2 cell-specific regulatory function. Although the majority of TE changes are identified in the AT2 cells, the AM cells also show TEs association with metalloproteases (MMP7 and 14), interleukin (IL15RA), chemokine (CCL22), and osteopontin (SPP1), which are all implicated in the development of IPF [43].

While expression of these immune-related genes (e.g., CCL22, IL15RA) is correlated with locus-specific TE expression in AM cells, their regulation can also be a consequence of downstream regulation caused by

inflammation in AT2 cells. The AM are also crucial players in respiratory system defense that involves the absorption of harmful particles and infectious agents [57]. Such processes could trigger genome instability (i.e. demethylation) and also directly activate TEs and their adjacent genes in AM.

The TE locus expression changes in our study that are associated with the adjacent gene expression are mainly located in either the 3'UTR, intronic, or 5'UTR region of the respective genes. Previous studies have shown that TEs can be found in gene regions and impact gene regulation by acting as, or interfering with, the regulatory elements in different tissue [58]. In particular, the SINE (Alu) elements that we identify as commonly embedded and expressed in the 3'UTR region are preferentially located in gene-rich regions due to their size (300 bp). The embedded Alu sequences can regulate the translation of their host genes acting as cis elements, or they can be involved in the microRNA regulatory network and many other regulatory process [59]. The role of these sequences in regulating the genes within lung cells as well as their relationship with disease have yet to be determined.

TEs are sometimes retained within introns and transcribed before the transcripts are processed, or else they are sometimes not spliced out at all, as indicated by a detailed study of the LINE elements [60]. The TEs retained within introns might result from non-preprocessed RNA and so might represent transcriptional noise rather than a biological signal. Thus, it must be noted that our study has limitations related to the quantification of authentic, independently transcribed TE loci.

The significant association that we have identified do not inevitably mean that a given TE indeed has a dominant effect on the transcription of the nearby gene. Transcriptional change of a given gene could also affect the expression of the nearby TEs, or TEs might not have an effect on gene expression at all as gene expression might be the result of downstream regulation [37, 38]. Thus, functional validation of identified candidate loci should be performed. Aside from these limitations, we could detect specific signals in the AT2 and AM cells that might be relevant to IPF and that were repeated in the single-cell data analysis. *In addition, although only a small number of patients were examined, our profiling of the three cell types obtained from the same patients suggests the strongest signal to occur in the AT2 cells, which are known to be injured in IPF. This study, therefore, identifies numerous candidate loci for further functional studies.*

Finally, smoking has been identified as an important risk factor for the development of IPF [61]. Interestingly, our GO term analysis of the TE loci-associated gene expression highlighted the enrichment of a few genes (eight out of 111,  $p < 0.0178$ ) in an earlier study [62]. This earlier study compared the gene expression of the small airway epithelium (SAE) cells of smokers and non-smokers, and it found that the eight genes (i.e., GSTA2, ITGA2, KRT19, MS4A8, MUC20, MUC5B, SCGB1A1, and SNTN) seen to correlate

with TE expression in our current study were also dysregulated in smokers. The SAE is the primary area where the early appearances of the majority of smoking-induced lung diseases are noted [63]. Thus, our observation might suggest that oxidative stress from cigarette smoke also represents an important TE-activating agent [64], and further, that it could be important during the very early stage of IPF development, a hypothesis that should be further tested.

## Conclusion

Taken together, our findings suggest a strong link between TE expression and processes known to be key to IPF. Yet, the extent to which the dysregulation of TEs drives IPF, or whether TE activation represents a side effect of pathogenesis, remains unclear. It is, however, tempting to speculate that a combination of TE demethylation due to aging (loss of epigenetic marks) and injury (oxidative stress) accompanied by dysfunctional autophagy can lead to perpetual inflammation and to changes in locus-specific gene expression, which might play a critical role in the development of IPF in genetically predisposed individuals. *In addition, our findings indicate potential new venues for therapies. Moreover, they call into question the role of TEs in other lung conditions caused by injury and inflammation (e.g., chronic obstructive pulmonary disease).*

## Materials And Methods

### ***Data***

*A detailed description of the samples has been previously published and is provided in Supplemental Table 1 [18].* We used samples from 14 donors and eight pulmonary fibrosis patients for which bulk RNA sequencing data concerning the AT2, AM, and WL cells were available. Briefly put, RNA was extracted and RNA-Seq libraries were prepared using a poly(A) enrichment (NEBNext Ultra RNA, New England BioLabs) and sequenced as single-end 75 base pair reads (Illumina NextSeq 500). We also analyzed single-cell data set from separately obtained eight donors and eight IPF patients from the same study. This data was generated using 3' V2 chemistry kit on Chromium Single cell controller (10x Genomics) and sequenced (Illumina HiSeq 4000). All the methods used for sample processing and sequencing have previously been described [18].

### **Quantification of the gene expression and TE activity using bulk RNA-seq**

*The raw sequencing data were downloaded from the dbGAP database (phs001750.v1.p1) and then processed using the SQUIRE set of tools, which integrates the alignment and expression counts for the gene expression and TE expression [26]. We mapped the raw RNA-seq reads to the GRCh38/hg38 (Dec. 2013 release) version of the human genome assembly, which was downloaded from the UCSC Genome FTP site (<ftp://hgdownload.cse.ucsc.edu/goldenPath/hg38/bigZips/chromFa.tar.gz>), and determined the transcriptional changes based on both the TE family and TE locus. To confirm the observed changes with*

the *SQUIRE*, we also quantified the TE expression using the *REdiscoverTE* set of tools (<http://research-pub.gene.com/REdiscoverTEpaper/>) [20]. *REdiscoverTE* was also used to determine the *transcriptional changes on the basis of the TE family separated by genomic region (intronic, exonic, and intergenic)*. The advantage of *REdiscoverTE* is that it can specifically model autonomous TE expression. To compare the two methods (*REdiscoverTE* and *SQUIRE*) for genomic-region-level analysis, we used *REdiscoverTE*-based annotation for the exonic, intronic, and intragenic regions and added up the reads obtained by *SQUIRE* per individual locus. This allowed us to compare the differential expression of the aggregated TE families in the genomic regions for the two methods. For both of these TE quantification methods, we used the same downstream approaches to determine the differentially expressed TE families.

*The counts were normalized between the samples, and the differential TEs expression between the healthy donors and the IPF patients in AT2, AM and WL cells was determined using the DESeq2 package in R. Significance of the TE expression was further determined using the Benjamini and Hochberg (BH)-adjusted p-value [65]. The volcano plots were constructed using the ggplot2 function in R.*

To identify the genomic locations of the differentially expressed TE loci in the cells, we downloaded the bed file annotation for the 3'UTR, 5'UTR, intron, and exon regions for each individual gene from the UCSC database table [66]. We further intersected the TE bed file coordinates of our differentially upregulated TEs with the different genomic regions using the *GenomicRanges* [67] package in R. Lastly, we identified the locations of the intergenic regions (those without overlap in 3'UTR, 5'UTR, intron, and exon regions) of the differentially expressed TEs and their distance from the nearest genes using the BEDTOOLS function *closest* [68].

## **Association between gene expression and TE expression**

We first correlated relationship between the L1HS subfamily and the differentially expressed TE-related genes (manually curated list of genes including type I interferons (IFN-I, 84 genes), senescence-associated secretory phenotype (SASP) genes (85 genes), L1 transcriptional regulator genes (two genes), and L1 post-transcriptional regulator genes (17 genes) [6, 29] using linear model (lm) function in R. The difference between the IPF and the donor groups for this relationship was further tested using F-test with *aov* function in R where TE subfamily expression represented the independent variable, and gene expression the dependent variable.

To determine whether the TE expression is related to the adjacent gene expression, we tested the correlation between the TEs located in the intergenic regions and those located within the 5'UTR, 3'UTR, and intron regions using a linear model in which the TE expression in each locus was modeled as the independent variable and the gene expression as the dependent variable, accounting for the phenotype

(IPF or donor) as a factor. The TEs that overlapped with the exons or that were located within the exon-intron, exon-5'UTR, or exon 3'UTR regions were excluded from these analyses. We only tested the cis TE-gene pairs, as most of the TEs were either within 50 kb of the gene or within gene regions. We defined the significant TE-gene pairs using the multiple test correction, BH-adjusted p-value [65]. The same tests were performed for the AT2, AM, and WL data. Difference between the

the regression slopes in groups (IPF or donor) was determined using F-test with *aov* function in R. Results were plotted using *ggplot2* function in R.

When the expression of more than one TE adjacent (within 50 kb distance) to the gene of interest was associated with the gene expression, we calculated the relative importance of each TE using the R package *relaimpo* and 1000 bootstraps [69]. We further tested for the gene ontology enrichment of the genes that were associated with TE expression using the STRING database [70].

## Detection of TE activity by means of scRNA-seq

### *Single-cell transcript mapping*

The raw reads of the single-cell RNA-seq data were downloaded from dbGAP (phs001750.v1.p1) [18].

The TE annotation library was downloaded using the *SQUIRE* package in R and the GRCh38/hg38 (Dec. 2013 release) genome, together with the TE reference. The genome-TE reference was built and the reads were mapped to both the genes and TE subfamilies using Chromium 10x workflow and the Chromium 10x Cell Ranger Single-Cell Software Suite (<http://software.10xgenomics.com/single-cell>).

The subfamily of TEs represents groups of sequences from the TE family (LINE, SINE, and LTRs) that are sufficiently distinct in terms of their repeats to allow for unique read mapping. Only the unique alignments were considered and counted for the differential expression analysis. The number of differences is defined as the number of TE subfamilies. The cell tags were matched with the published data matrix so that the same cells were used as in previously published accounts [18]. The filtered feature matrices produced by the cell ranger were used in the subsequent analysis using the R package *Seurat* [71].

### *ScRNA-seq clustering*

The downstream single-cell analysis was performed using functions in both the *Seurat* package V3 and R 3.5 [71]. First, we matched the cells of eight healthy donors and eight IPF patients from our alignment counts to the published filtered dataset available at GEO (GSE122960) [18]. In doing so, we recovered a total of 77,517 cells. To compare the expression data from different patients and different lung cell types, we integrated the data with the *IntegrateData* function and identified the anchors between the dataset using the *FindIntegrationAnchors* function. The normalization of the 22,009 identified genes was performed based on the total number of unique molecular identifiers (UMIs) per cells, multiplied by a scale factor (10,000) and then log transformed. We next conducted a principal component analysis (PCA) of the top 2000 variable genes and then used the first 20 PCA components to project the cells onto a two-dimensional map using the uniform manifold approximation and projection (UMAP) dimensionally reduction method offered by the *RunUMAP* function. To identify the cell types from the lung tissue, we clustered all the IPF patient and donor cells using the K-nearest neighbor (KNN) graph-based clustering algorithm and the *FindNeighbors* function. Finally, we used the *FindClusters* function (resolution parameter = 0.5) to establish the cell clusters, while the cluster identity was determined based on the conventional cell marker genes [18, 44]. The differential gene and TE subfamilies expression analysis between the IPF patients and the donors was performed for each cell type using the non-parametric Wilcoxon rank-sum test and the Bonferroni correction. In addition, we compared the IPF patients to the donors in terms of the total expression of the L1 TE subfamilies per cell (L1 score) using the *addModuleScore* function and the Wilcoxon rank-sum test. To calculate the L1 score per cell, we used the average expression of 70 L1 subfamilies. We next tested whether the relationship between the L1 score and the TE related genes (126 genes known to be part of the L1 defense and antiviral interferon-stimulating genes identified in RNA bulk sequencing) differed between AT2 cells of the IPF patients and the donors. A linear model was fitted for each L1 score and the gene pairs for the IPF patients and the donors using the *lm* function in R, while the difference between the regression lines of two groups was determined using the t-test and *aov* function in R.

## Declarations

### Acknowledgments

We wish to thank dbGap and Reyfman *et al.* [18] for making this data available. The origin of this dataset is described comprehensively in a manuscript found at

<https://www.atsjournals.org/doi/10.1164/rccm.201712-2410OC>. We would like to thank all the institutions and founding agencies that participated in the data collection as described below. This research was supported in part by The Veterans Administration Grant BX000201 and Department of Defense grant PR141319. We would like to acknowledge the Ernest S. Bazley Professorship in Airway Diseases and the Mabel Greene Myers Professorship in Medicine-Rheumatology at the Northwestern University Feinberg School of Medicine. This research was supported in part through the computational resources and staff contributions provided by the Genomics Computing Cluster (Genomic Nodes on Quest) which is jointly supported by the Feinberg School of Medicine, the Center for Genetic Medicine, and Feinberg's Department of Biochemistry and Molecular Genetics, the Office of the Provost, the Office

for Research, and Northwestern Information Technology. The Genomics Computing Cluster is part of Quest, Northwestern University's high-performance computing facility, with the purpose to advance research in genomics. Next generation sequencing on the Illumina HiSeq 4000 was performed by the NUSeq Core Facility, which is supported by the Northwestern University Center for Genetic Medicine, Feinberg School of Medicine, and Shared and Core Facilities of the University's Office for Research. Northwestern University Flow Cytometry Facility, Center for Advanced Microscopy, and Pathology Core Facility are supported by NCI Cancer Center Support Grant P30 CA060553 awarded to the Robert H Lurie Comprehensive Cancer Center.

### **Ethics approval and consent to participate**

Not applicable.

### **Consent for publication**

Not applicable.

### **Availability of data and materials**

All data generated or analyzed during this study are included in Reyfman *et al.* [18] published article and its supplementary information files. Raw genomics reads and detailed patient data are available from the GSE122960 dataset and from the *dbGAP database* (phs001750.v1.p1), although restrictions apply with regard to the availability due to *dbGAP policy*. *Data access was obtained from dbGAP*

(Project #21807).

## **Funding**

*Mahboubeh R. Rostami was supported by T32 HL094284.*

### **Competing interests**

The authors declare that they have no competing interests

## **Author contributions**

M.B. designed the study, performed data analyses, and wrote the manuscript. M.R. performed single cell data analysis and wrote the manuscript. All authors read and approved the final manuscript.

## **References**

1. Seberg O, Petersen G: **A unified classification system for eukaryotic transposable elements should reflect their phylogeny.** *Nat Rev Genet* 2009, **10**(4):276-276.

2. Lander ES, Linton LM, Birren B, Nusbaum C, Zody MC, Baldwin J, Devon K, Dewar K, Doyle M, FitzHugh W *et al*: **Initial sequencing and analysis of the human genome.** *Nature* 2001, **409**(6822):860-921.
3. Mills RE, Bennett EA, Iskow RC, Devine SE: **Which transposable elements are active in the human genome?** *Trends Genet* 2007, **23**(4):183-191.
4. Feschotte C: **Transposable elements and the evolution of regulatory networks.** *Nat Rev Genet* 2008, **9**(5):397-405.
5. Bourque G, Burns KH, Gehring M, Gorbunova V, Seluanov A, Hammell M, Imbeault M, Izsvak Z, Levin HL, Macfarlan TS *et al*: **Ten things you should know about transposable elements.** *Genome Biol* 2018, **19**(1):199.
6. De Cecco M, Ito T, Petrashen AP, Elias AE, Skvir NJ, Criscione SW, Caligiana A, Broccoli G, Adney EM, Boeke JD *et al*: **L1 drives IFN in senescent cells and promotes age-associated inflammation.** *Nature* 2019, **566**(7742):73-78.
7. Simon M, Van Meter M, Ablaeva J, Ke Z, Gonzalez RS, Taguchi T, De Cecco M, Leonova KI, Kogan V, Helfand SL *et al*: **LINE1 Derepression in Aged Wild-Type and SIRT6-Deficient Mice Drives Inflammation.** *Cell Metab* 2019, **29**(4):871-885 e875.
8. Goodier JL, Kazazian HH, Jr.: **Retrotransposons revisited: the restraint and rehabilitation of parasites.** *Cell* 2008, **135**(1):23-35.
9. Baylin SB, Herman JG, Graff JR, Vertino PM, Issa JP: **Alterations in DNA methylation: a fundamental aspect of neoplasia.** *Adv Cancer Res* 1998, **72**:141-196.
10. Deniz O, Frost JM, Branco MR: **Author Correction: Regulation of transposable elements by DNA modifications.** *Nat Rev Genet* 2019, **20**(7):432.
11. Saleh A, Macia A, Muotri AR: **Transposable Elements, Inflammation, and Neurological Disease.** *Front Neurol* 2019, **10**:894.
12. Sargurupremraj M, Wjst M: **Transposable elements and their potential role in complex lung disorder.** *Respir Res* 2013, **14**:99.
13. Barratt SL, Creamer A, Hayton C, Chaudhuri N: **Idiopathic Pulmonary Fibrosis (IPF): An Overview.** *J Clin Med* 2018, **7**(8).
14. Kaur A, Mathai SK, Schwartz DA: **Genetics in Idiopathic Pulmonary Fibrosis Pathogenesis, Prognosis, and Treatment.** *Front Med (Lausanne)* 2017, **4**:154.
15. Wynn TA, Ramalingam TR: **Mechanisms of fibrosis: therapeutic translation for fibrotic disease.** *Nat Med* 2012, **18**(7):1028-1040.
16. Camelo A, Dunmore R, Sleeman MA, Clarke DL: **The epithelium in idiopathic pulmonary fibrosis: breaking the barrier.** *Front Pharmacol* 2014, **4**:173.
17. Giorgi G, Marcantonio P, Del Re B: **LINE-1 retrotransposition in human neuroblastoma cells is affected by oxidative stress.** *Cell Tissue Res* 2011, **346**(3):383-391.

18. Reyfman PA, Walter JM, Joshi N, Anekalla KR, McQuattie-Pimentel AC, Chiu S, Fernandez R, Akbarpour M, Chen CI, Ren Z *et al*: **Single-Cell Transcriptomic Analysis of Human Lung Provides Insights into the Pathobiology of Pulmonary Fibrosis**. *Am J Respir Crit Care Med* 2019, **199**(12):1517-1536.
19. Mehta CR, Patel NR, Tsiatis AA: **Exact significance testing to establish treatment equivalence with ordered categorical data**. *Biometrics* 1984, **40**(3):819-825.
20. Kong Y, Rose CM, Cass AA, Williams AG, Darwish M, Lianoglou S, Haverty PM, Tong AJ, Blanchette C, Albert ML *et al*: **Transposable element expression in tumors is associated with immune infiltration and increased antigenicity**. *Nat Commun* 2019, **10**(1):5228.
21. Schafer MJ, White TA, Iijima K, Haak AJ, Ligresti G, Atkinson EJ, Oberg AL, Birch J, Salmonowicz H, Zhu Y *et al*: **Cellular senescence mediates fibrotic pulmonary disease**. *Nat Commun* 2017, **8**:14532.
22. Faner R, Rojas M, Macnee W, Agusti A: **Abnormal lung aging in chronic obstructive pulmonary disease and idiopathic pulmonary fibrosis**. *Am J Respir Crit Care Med* 2012, **186**(4):306-313.
23. Lehmann M, Korfei M, Mutze K, Klee S, Skronska-Wasek W, Alsafadi HN, Ota C, Costa R, Schiller HB, Lindner M *et al*: **Senolytic drugs target alveolar epithelial cell function and attenuate experimental lung fibrosis ex vivo**. *Eur Respir J* 2017, **50**(2).
24. Sisson TH, Mendez M, Choi K, Subbotina N, Courey A, Cunningham A, Dave A, Engelhardt JF, Liu X, White ES *et al*: **Targeted injury of type II alveolar epithelial cells induces pulmonary fibrosis**. *Am J Respir Crit Care Med* 2010, **181**(3):254-263.
25. Yao C, Guan X, Carraro G, Parimon T, Liu X, Huang G, Mulay A, Soukiasian HJ, David G, Weigt SS *et al*: **Senescence of Alveolar Type 2 Cells Drives Progressive Pulmonary Fibrosis**. *Am J Respir Crit Care Med* 2020.
26. Yang WR, Ardeljan D, Pacyna CN, Payer LM, Burns KH: **SQUIRE reveals locus-specific regulation of interspersed repeat expression**. *Nucleic Acids Res* 2019, **47**(5):e27.
27. Jurka J, Bao W, Kojima KK: **Families of transposable elements, population structure and the origin of species**. *Biol Direct* 2011, **6**:44.
28. Brouha B, Schustak J, Badge RM, Lutz-Prigge S, Farley AH, Moran JV, Kazazian HH, Jr.: **Hot L1s account for the bulk of retrotransposition in the human population**. *Proc Natl Acad Sci U S A* 2003, **100**(9):5280-5285.
29. Goodier JL: **Restricting retrotransposons: a review**. *Mob DNA* 2016, **7**:16.
30. Jung H, Choi JK, Lee EA: **Immune signatures correlate with L1 retrotransposition in gastrointestinal cancers**. *Genome Res* 2018, **28**(8):1136-1146.
31. Heukels P, Moor CC, von der Thusen JH, Wijsenbeek MS, Kool M: **Inflammation and immunity in IPF pathogenesis and treatment**. *Respir Med* 2019, **147**:79-91.
32. Lunardi F, Villano G, Perissinotto E, Agostini C, Rea F, Gnoato M, Bradaschia A, Valente M, Pontisso P, Calabrese F: **Overexpression of SERPIN B3 promotes epithelial proliferation and lung fibrosis in mice**. *Lab Invest* 2011, **91**(6):945-954.

33. Guo H, Chitiprolu M, Gagnon D, Meng L, Perez-Iratxeta C, Lagace D, Gibbins D: **Autophagy supports genomic stability by degrading retrotransposon RNA.** *Nat Commun* 2014, **5**:5276.
34. Yu Q, Carbone CJ, Katlinskaya YV, Zheng H, Zheng K, Luo M, Wang PJ, Greenberg RA, Fuchs SY: **Type I interferon controls propagation of long interspersed element-1.** *J Biol Chem* 2015, **290**(16):10191-10199.
35. Jiang C, Liu G, Luckhardt T, Antony V, Zhou Y, Carter AB, Thannickal VJ, Liu RM: **Serpine 1 induces alveolar type II cell senescence through activating p53-p21-Rb pathway in fibrotic lung disease.** *Aging Cell* 2017, **16**(5):1114-1124.
36. Yamashita CM, Dolgonos L, Zemans RL, Young SK, Robertson J, Briones N, Suzuki T, Campbell MN, Gauldie J, Radisky DC *et al*: **Matrix metalloproteinase 3 is a mediator of pulmonary fibrosis.** *Am J Pathol* 2011, **179**(4):1733-1745.
37. Lanciano S, Cristofari G: **Measuring and interpreting transposable element expression.** *Nat Rev Genet* 2020, **21**(12):721-736.
38. Karakulah G, Arslan N, Yandim C, Suner A: **TEffectR: an R package for studying the potential effects of transposable elements on gene expression with linear regression model.** *PeerJ* 2019, **7**:e8192.
39. Martinez FJ, Collard HR, Pardo A, Raghu G, Richeldi L, Selman M, Swigris JJ, Taniguchi H, Wells AU: **Idiopathic pulmonary fibrosis.** *Nat Rev Dis Primers* 2017, **3**:17074.
40. Seibold MA, Wise AL, Speer MC, Steele MP, Brown KK, Loyd JE, Fingerlin TE, Zhang W, Gudmundsson G, Groshong SD *et al*: **A common MUC5B promoter polymorphism and pulmonary fibrosis.** *N Engl J Med* 2011, **364**(16):1503-1512.
41. Hunninghake GM, Hatabu H, Okajima Y, Gao W, Dupuis J, Latourelle JC, Nishino M, Araki T, Zazueta OE, Kurugol S *et al*: **MUC5B promoter polymorphism and interstitial lung abnormalities.** *N Engl J Med* 2013, **368**(23):2192-2200.
42. Yogo Y, Fujishima S, Inoue T, Saito F, Shiomi T, Yamaguchi K, Ishizaka A: **Macrophage derived chemokine (CCL22), thymus and activation-regulated chemokine (CCL17), and CCR4 in idiopathic pulmonary fibrosis.** *Respir Res* 2009, **10**:80.
43. Pardo A, Cabrera S, Maldonado M, Selman M: **Role of matrix metalloproteinases in the pathogenesis of idiopathic pulmonary fibrosis.** *Respir Res* 2016, **17**:23.
44. Reyfman PA, Walter JM, Joshi N, Anekalla KR, McQuattie-Pimentel AC, Chiu S, Fernandez R, Akbarpour M, Chen CI, Ren ZY *et al*: **Single-Cell Transcriptomic Analysis of Human Lung Provides Insights into the Pathobiology of Pulmonary Fibrosis.** *Am J Resp Crit Care* 2019, **199**(12):1517-1536.
45. Sharma R, Rodic N, Burns KH, Taylor MS: **Immunodetection of Human LINE-1 Expression in Cultured Cells and Human Tissues.** *Methods Mol Biol* 2016, **1400**:261-280.
46. Payer LM, Burns KH: **Transposable elements in human genetic disease.** *Nat Rev Genet* 2019.
47. Chuong EB, Elde NC, Feschotte C: **Regulatory activities of transposable elements: from conflicts to benefits.** *Nat Rev Genet* 2017, **18**(2):71-86.

48. Hill C, Li J, Liu D, Conforti F, Brereton CJ, Yao L, Zhou Y, Alzetani A, Chee SJ, Marshall BG *et al*: **Autophagy inhibition-mediated epithelial-mesenchymal transition augments local myofibroblast differentiation in pulmonary fibrosis.** *Cell Death Dis* 2019, **10**(8):591.
49. Agostini C, Gurrieri C: **Chemokine/cytokine cocktail in idiopathic pulmonary fibrosis.** *Proc Am Thorac Soc* 2006, **3**(4):357-363.
50. Raghu G, Weycker D, Edelsberg J, Bradford WZ, Oster G: **Incidence and prevalence of idiopathic pulmonary fibrosis.** *Am J Respir Crit Care Med* 2006, **174**(7):810-816.
51. Pal S, Tyler JK: **Epigenetics and aging.** *Sci Adv* 2016, **2**(7):e1600584.
52. Parimon T, Yao C, Stripp BR, Noble PW, Chen P: **Alveolar Epithelial Type II Cells as Drivers of Lung Fibrosis in Idiopathic Pulmonary Fibrosis.** *Int J Mol Sci* 2020, **21**(7).
53. Helling BA, Gerber AN, Kadiyala V, Sasse SK, Pedersen BS, Sparks L, Nakano Y, Okamoto T, Evans CM, Yang IV *et al*: **Regulation of MUC5B Expression in Idiopathic Pulmonary Fibrosis.** *Am J Respir Cell Mol Biol* 2017, **57**(1):91-99.
54. Wang Y, Yella J, Chen J, McCormack FX, Madala SK, Jegga AG: **Unsupervised gene expression analyses identify IPF-severity correlated signatures, associated genes and biomarkers.** *BMC Pulm Med* 2017, **17**(1):133.
55. Criscione SW, Theodosakis N, Micevic G, Cornish TC, Burns KH, Neretti N, Rodic N: **Genome-wide characterization of human L1 antisense promoter-driven transcripts.** *BMC Genomics* 2016, **17**:463.
56. Wang Z, Zhu J, Chen F, Ma L: **Weighted Gene Coexpression Network Analysis Identifies Key Genes and Pathways Associated with Idiopathic Pulmonary Fibrosis.** *Med Sci Monit* 2019, **25**:4285-4304.
57. Thorley AJ, Ford PA, Giembycz MA, Goldstraw P, Young A, Tetley TD: **Differential regulation of cytokine release and leukocyte migration by lipopolysaccharide-stimulated primary human lung alveolar type II epithelial cells and macrophages.** *J Immunol* 2007, **178**(1):463-473.
58. Garcia-Perez JL, Widmann TJ, Adams IR: **The impact of transposable elements on mammalian development.** *Development* 2016, **143**(22):4101-4114.
59. Chen LL, Yang L: **ALU alternative Regulation for Gene Expression.** *Trends Cell Biol* 2017, **27**(7):480-490.
60. Deininger P, Morales ME, White TB, Baddoo M, Hedges DJ, Servant G, Srivastav S, Smither ME, Concha M, DeHaro DL *et al*: **A comprehensive approach to expression of L1 loci.** *Nucleic Acids Res* 2017, **45**(5):e31.
61. Baumgartner KB, Samet JM, Stidley CA, Colby TV, Waldron JA: **Cigarette smoking: a risk factor for idiopathic pulmonary fibrosis.** *Am J Respir Crit Care Med* 1997, **155**(1):242-248.
62. Hackett NR, Butler MW, Shaykhiev R, Salit J, Omberg L, Rodriguez-Flores JL, Mezey JG, Strulovici-Barel Y, Wang G, Didon L *et al*: **RNA-Seq quantification of the human small airway epithelium transcriptome.** *BMC Genomics* 2012, **13**:82.
63. Hogg JC, Chu F, Utokaparch S, Woods R, Elliott WM, Buzatu L, Cherniack RM, Rogers RM, Sciurba FC, Coxson HO *et al*: **The nature of small-airway obstruction in chronic obstructive pulmonary disease.** *N Engl J Med* 2004, **350**(26):2645-2653.

64. Bollati V, Baccarelli A, Hou L, Bonzini M, Fustinoni S, Cavallo D, Byun HM, Jiang J, Marinelli B, Pesatori AC *et al*: **Changes in DNA methylation patterns in subjects exposed to low-dose benzene.** *Cancer Res* 2007, **67**(3):876-880.
65. Love MI, Huber W, Anders S: **Moderated estimation of fold change and dispersion for RNA-seq data with DESeq2.** *Genome Biol* 2014, **15**(12):550.
66. Karolchik D, Hinrichs AS, Furey TS, Roskin KM, Sugnet CW, Haussler D, Kent WJ: **The UCSC Table Browser data retrieval tool.** *Nucleic Acids Res* 2004, **32**(Database issue):D493-496.
67. Lawrence M, Huber W, Pages H, Aboyoun P, Carlson M, Gentleman R, Morgan MT, Carey VJ: **Software for computing and annotating genomic ranges.** *PLoS Comput Biol* 2013, **9**(8):e1003118.
68. Quinlan AR, Hall IM: **BEDTools: a flexible suite of utilities for comparing genomic features.** *Bioinformatics* 2010, **26**(6):841-842.
69. Grömping U: **Relative Importance for Linear Regression in R: The Package relaimpo.** . *Journal of Statistical Software* 2006, **17**:1–27.
70. Szklarczyk D, Gable AL, Lyon D, Junge A, Wyder S, Huerta-Cepas J, Simonovic M, Doncheva NT, Morris JH, Bork P *et al*: **STRING v11: protein-protein association networks with increased coverage, supporting functional discovery in genome-wide experimental datasets.** *Nucleic Acids Res* 2019, **47**(D1):D607-D613.
71. Stuart T, Butler A, Hoffman P, Hafemeister C, Papalexi E, Mauck WM, 3rd, Hao Y, Stoeckius M, Smibert P, Satija R: **Comprehensive Integration of Single-Cell Data.** *Cell* 2019, **177**(7):1888-1902 e1821.

## Tables

**Table 1. Summary of all the identified genes and TE expression changes.**

Significant changes ( $p_{\text{adjusted}} < 0.05$ ) between the donors and IPF patients in the WL, AT2 and AM are shown.

A. Differential expression analysis of TEs families and genes in three cell types

	WL	AT2	AM	
TE Family	UP/DOWN	UP/DOWN	UP/DOWN	UP/DOWN
SINE	0/0	1/1	1/0	
LINE	0/4	17/2	0/1	
LTR	11/0	40/17	6/5	
Other	3/0	14/2	4/0	
<b>Genes</b>	654/516	2477/1654	566/467	

The TE changes are shown at the family level whereas each number represents number of TEs subfamily changes. WL: whole lung; AT2: alveolar type II cell; AM: alveolar macrophage.

B. Enrichment analysis of individual elements in three cell types

	Differential expression	No differential expression	Total in the genome	Fisher exact test of enrichment
<b>WL</b>				
LINE	4	179	183	0.75
LTR	11	577	588	0.75
SINE	0	63	63	0.61
<b>AT2</b>				
LINE	19	164	183	0.56
LTR	57	531	588	0.69
SINE	2	61	63	0.11
<b>AM</b>				
LINE	1	182	183	0.31
LTR	11	577	588	0.36
SINE	1	62	63	1.00

The TE changes are shown at the family level whereas each number represents number of TEs subfamily changes. WL: whole lung; AT2: alveolar type II cell; AM: alveolar macrophage. Enrichment analysis of individual families was performed using Fisher exact test where each family was tested against the sum of other families for each cell type. Only LINE, SINE and LTR families were considered.

**Table 2. Genomic distribution and gene ontology (GO) enrichment of genes significantly associated with TEs in the AT2 and AM cells.**

A. GO enrichment of genes significantly related to TEs expression. A gene ontology enrichment analysis was performed on those genes with significant cis TE associations using the STRING database [70]. The total number of observed and background genes in each GO term category as well as all false discovery rate values (FDR) < 0.05 are shown for the AT2 and AM cells.

<b>AT2</b>				
GO TERM	Description	observed gene count	background gene count	FDR
GO:0035082	axoneme assembly	6	59	0.0022
GO:0003341	cilium movement	5	61	0.009
GO:0060271	cilium assembly	10	326	0.009
GO:0070286	axonemal dynein complex assembly	4	32	0.009
GO:0120031	plasma membrane bounded cell projection assembly	11	413	0.009
GO:0036159	inner dynein arm assembly	3	16	0.0263
GO:0070925	organelle assembly	12	666	0.044
<b>AM</b>				
GO:0006955	immune response	16	1560	0.0163
GO:0045124	regulation of bone resorption	4	38	0.0163
GO:0002376	immune system process	19	2370	0.0282

B. Summary of genomic distribution of TE-genes cis loci pairs in AM and AT2 cells identified by linear model test. Number of significantly observed changes are shown per each genomic region.

AT2				
TE family	Intron	Intergenic	3'UTR3	5'UTR
SINE	30	5	38	1
LINE	26	3	26	0
LTR	14	4	11	1
Other	5	0	7	1
AM				
SINE	7	0	46	3
LINE	4	0	22	0
LTR	1	0	5	0
Other	1	0	14	1

## Figures

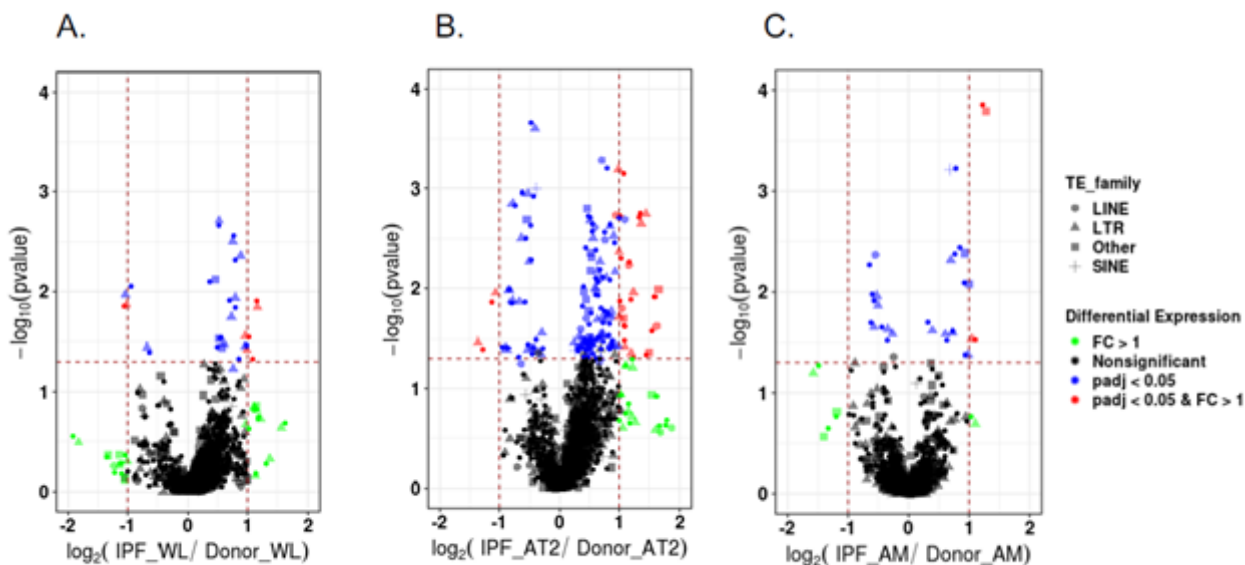


**Figure 1**

Changes in the expression of TE families in individual cell types and whole-lung tissue. A. Bulk RNA-seq of whole-lung tissue (WL). B. Bulk RNA-seq of flow cytometry-sorted alveolar type II cells (AT2). C. Bulk RNA-seq of flow cytometry-sorted alveolar macrophages (AM). The TE expression was determined by read counts using the SQuIRE suite of tools, while the differential expression analysis was performed using the DESeq2 package in R. The x-axis represents the log<sub>2</sub> ratio of the TE subfamily expression between the IPF patients and the donors. The y-axis represents the adjusted p-value based on -log<sub>10</sub>. The

red dots represent the TE subfamilies with a fold expression change (FC) > 1 and p.adjust < 0.05 (as represented by two vertical dotted lines). The blue dots represent the TEs with an adjusted p-value (p.adjust) < 0.05, while the green dots represent the TEs with an FC > 1. The black dots represent changes that do not have a significant p.adjust value or an FC higher than 1. Different shapes represent different TE families.

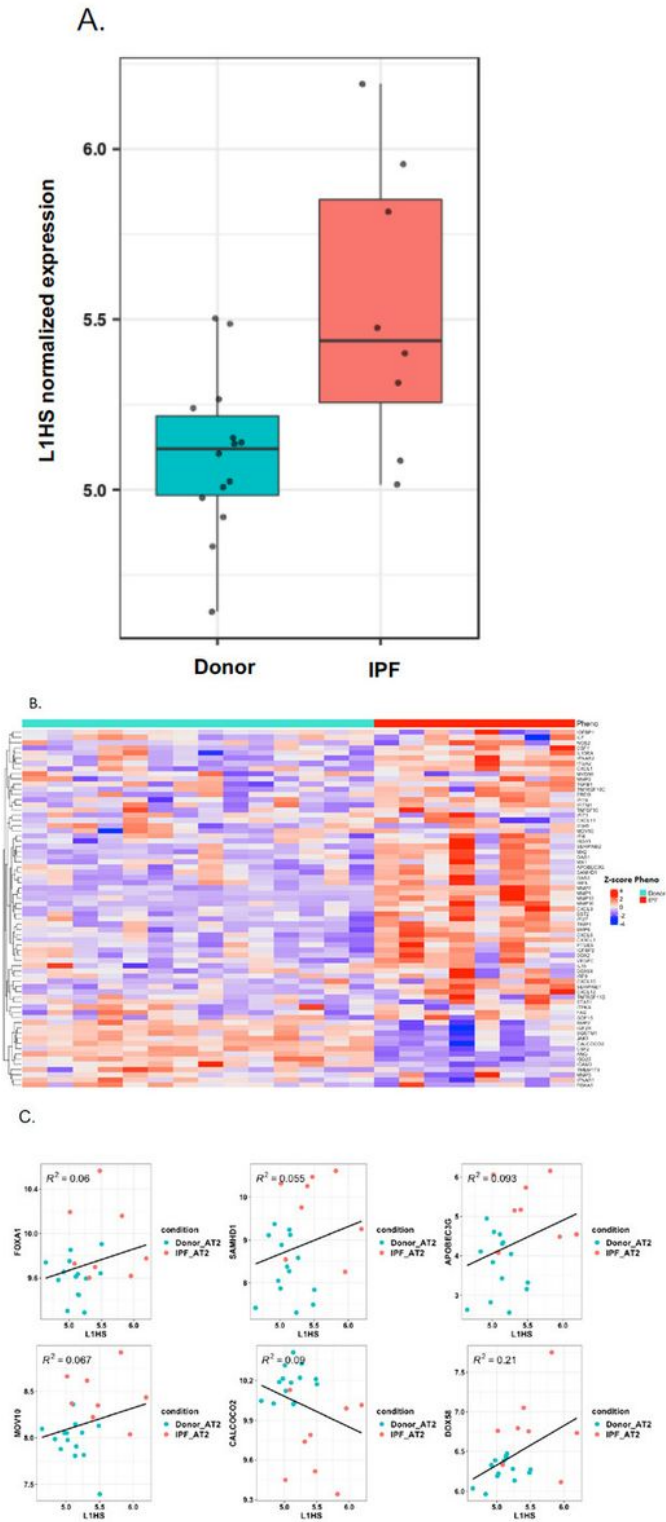
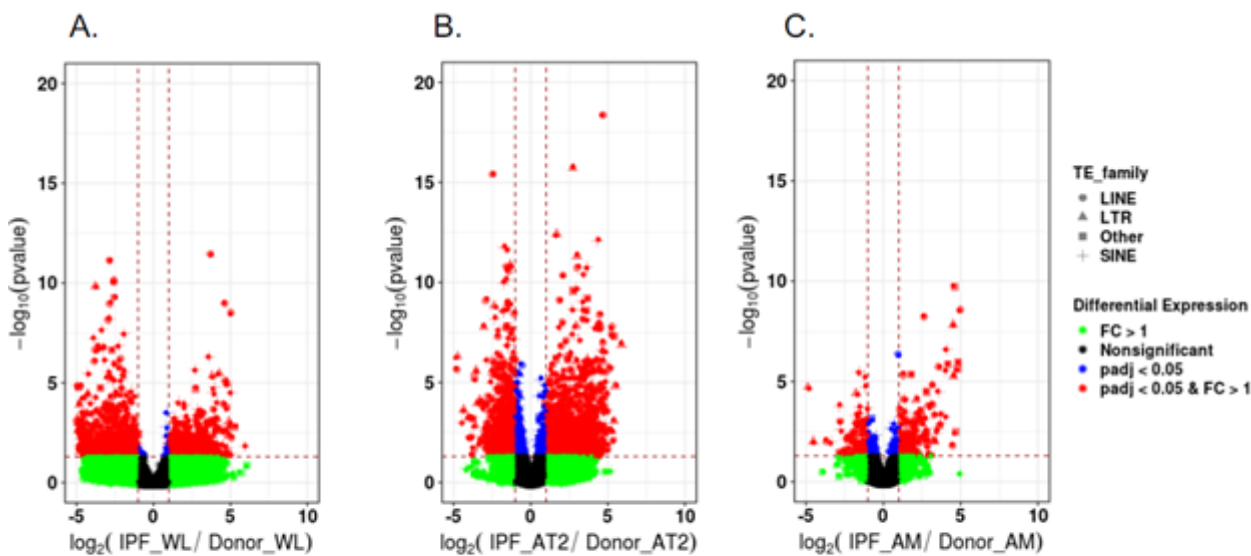


Figure 2

L1HS intergenic expression is associated with the IPF phenotype and expression of genes with functional relevance to L1HS activity. A. L1HS intergenic expression in Donor and IPF samples as quantified by RDiscoverTE method. Green: donor samples. Red: IPF samples. The x-axis represents groups; the y-axis represents log-normalized L1HS expression values. L1HS expression between the groups is significantly different as determined by DESeq2 analysis ( $p.adjust=0.001$ ). B. Heatmap of differentially expressed genes from four genes sets which are functionally relevant to L1HS activity [34, 68]: type I interferons (IFN-I, 84 genes), senescence-associated secretory phenotype genes (SASP, 85 genes), L1 transcriptional regulator genes (2 genes), and L1 post-transcriptional regulator genes (17 genes). The heatmap colors represent log-normalized gene expression (blue- low expression, red-high expression). The horizontal bars symbolize the four gene sets. Samples are grouped on the y-axis by their phenotypes. C. Examples of L1HS co-expression correlation with genes functionally relevant to L1HS activity from four gene sets: INF-I pathway (DDX58, IFI16, STAT1, IRF9, ISG15), senescence-associated secretory phenotype(SASP) genes (MMP3, SERPINE 1), L1 transcriptional regulator genes (FOXA1), and L1 post-transcriptional regulator genes (SAMHD1, MOV10, and APOBEC3G, CALCOCO2). Plots show the correlation of log-normalized gene expression (y-axis) and L1HS (x-axis) expression in the AT2 cells. The colors represent the phenotypes (Green: donor; Red: IPF). The R2 values from linear model fit each gene-L1HS relationship are shown. Results of all tested genes are summarized in (Supplemental Table 4B-C).



**Figure 3**

Differentially regulated TE loci in IPF patients vs. donors in cell types and whole-lung tissue. A. Bulk RNA-seq of whole-lung tissue. B. Bulk RNA-seq of flow cytometry-sorted alveolar type II cells (AT2). C. Bulk RNA-seq of flow cytometry-sorted alveolar macrophages (AM). The TE expression was determined by read counts using the SQuIRE suite of tools, while the differential expression analysis was performed using the DESeq2 package in R. The x-axis represents the log<sub>2</sub> ratio of the TE locus expression between

the IPF patients and donors. The y-axis represents the adjusted p-value based on  $-\log_{10}$ . The yellow dots represent the TE loci with a fold expression change (FC) > 1 and  $p_{\text{adjust}} < 0.05$  (as represented by two vertical dotted lines). The blue dots represent the TEs with an adjusted p-value ( $p_{\text{adjust}} < 0.05$ ), while the green dots represent the TEs with an FC > 1. The grey dots represent changes that do not have a significant  $p_{\text{adjust}}$  value change or an FC higher than 1.

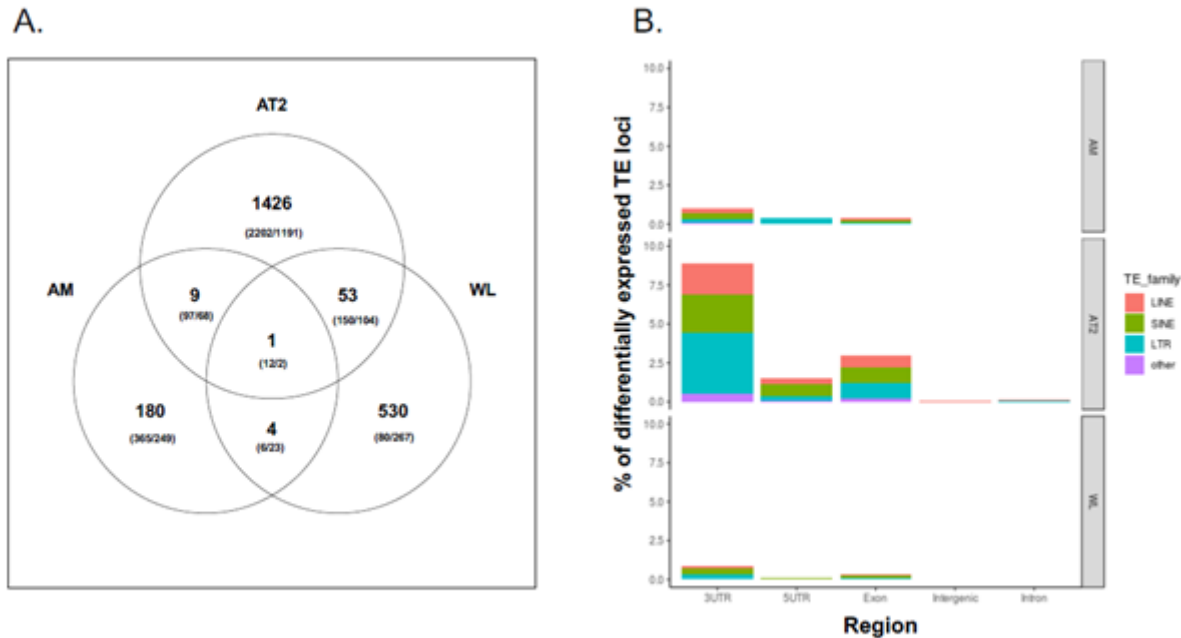


**Figure 4**

Summary of the IPF-associated TE loci changes and their association with the adjacent genes. A. A Venn diagram of the overlap between the upregulated TE loci in the IPF patients when compared with the donors in whole-lung tissue (WT), alveolar type II cells (AT2), and alveolar macrophages (AM) (upper number), with the overlap between the upregulated (first number in the brackets) and downregulated genes (second number in the brackets). B. Histograms summarizing the TE expression changes by intergenic and intragenic regions in the WL, AT2 and AM. The intragenic regions are divided into the 3'UTR, 5'UTR, intron, and exon regions. The different colors represent the proportion of each TE family in each region. The x-axis represents the individual genomic regions. The y-axis represents the percentage of TE loci per TE family that are normalized by the total number of each TE family present in each genomic region.

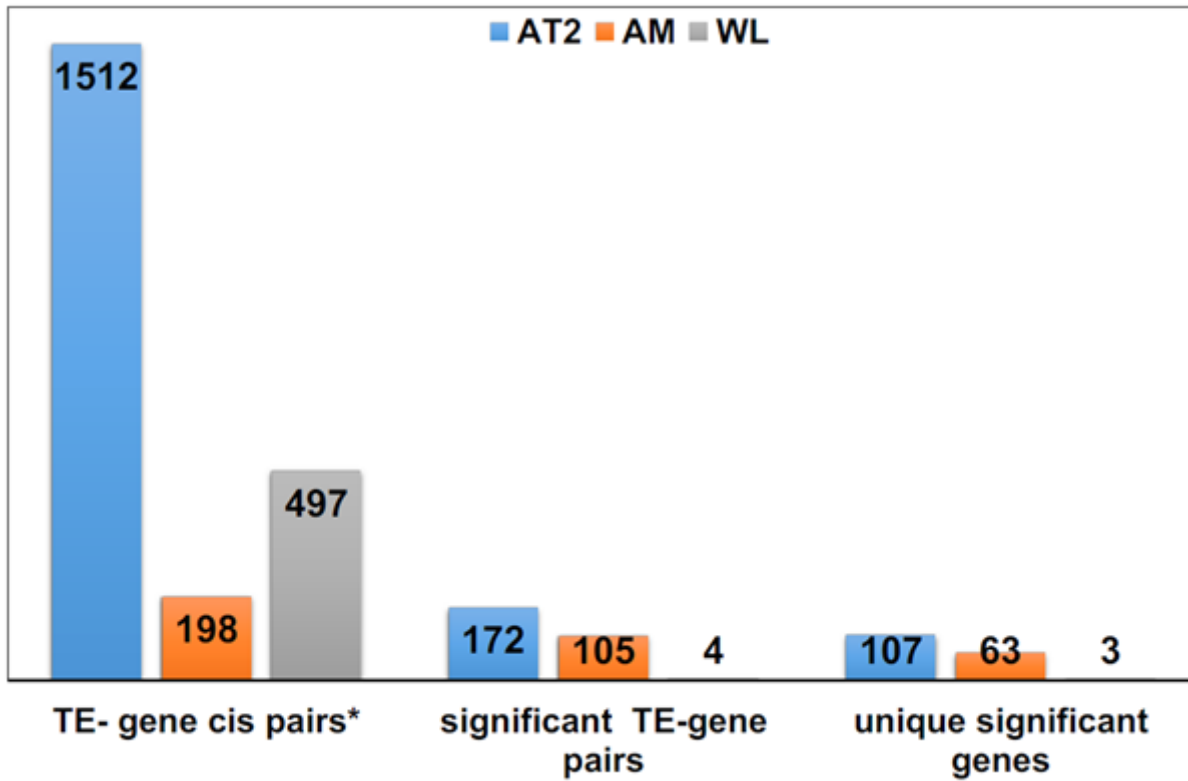


**Figure 5**

Barplots summarizing the TE-gene associations in the whole-lung tissue, AT2, and AM. The association between the log<sub>2</sub>-transformed TE expression (independent variable) and the log<sub>2</sub>-transformed gene expression (dependent variable) was tested using a linear model (lm). The p-value correction was performed using the Benjamini and Hochberg (BH) test. Only the expressions of significant genes and significantly upregulated TEs located next to the gene (max distance 50 kb) cis loci are summarized here.

Figure 6

A.

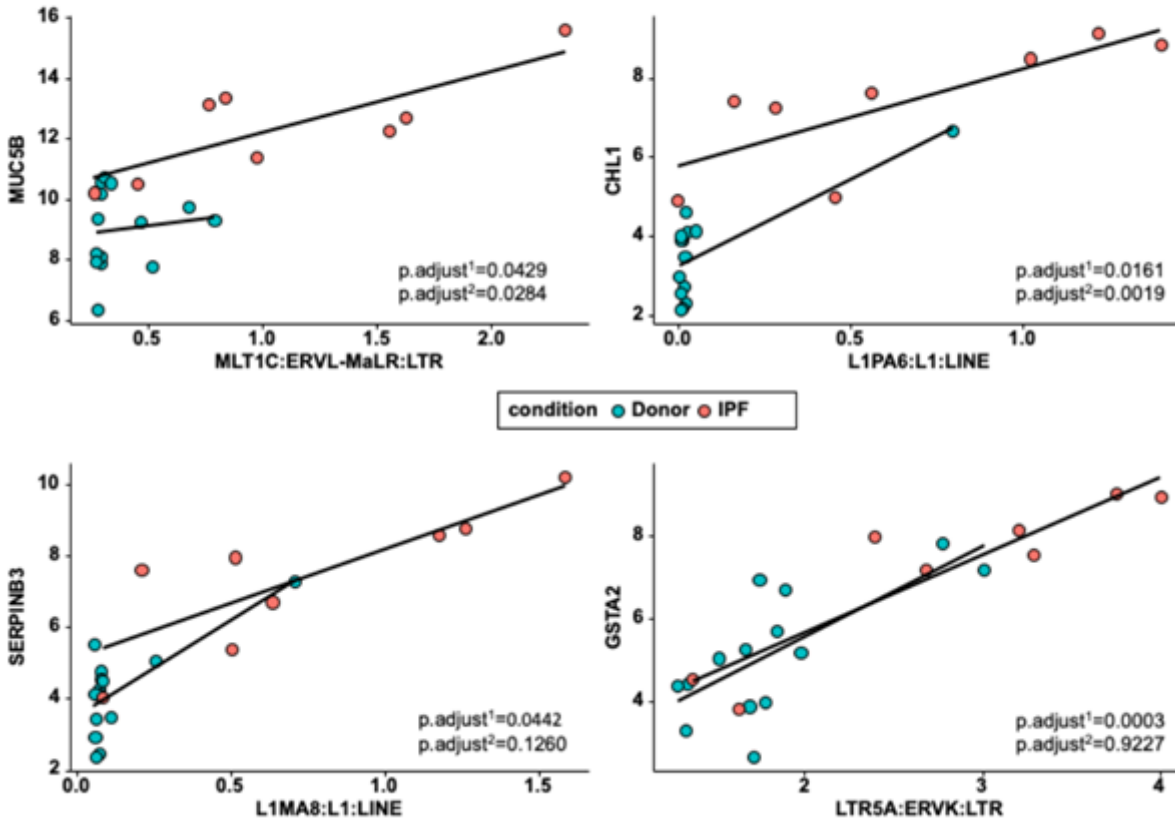
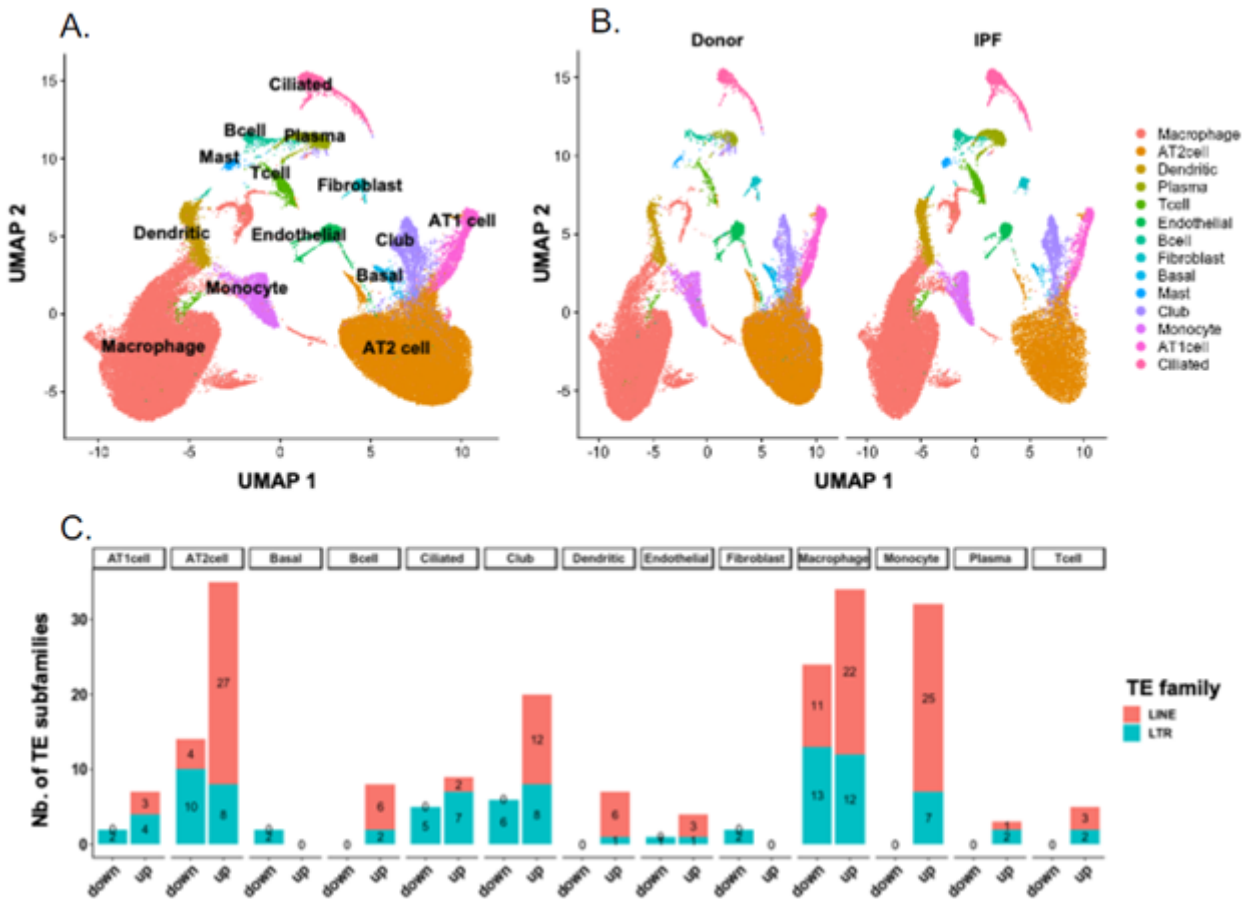


Figure 6

Examples of the gene expression correlation with the adjacent TE loci. A. Correlation plots representing the correlation between the MUC5B, CHL1, SERPINB3, and GSTA2 genes and the adjacent TE loci in the AT2 cells. B. Correlation plots representing the correlation of the CCL2, MMP7, IL1RN, SPP1, and genes and the TEs in the AM cells. The x-axis represents the normalized expression values for the TEs, while the y-axis represents the normalized expression values for the genes. The colors represent the phenotypes (Green: donor; Red: IPF patient). The BH p.adjusted values for each relationship are shown; p.adjust<sup>1</sup> represents relationship between gene expression and adjacent TE-locus expression, and p.adjust<sup>2</sup> represents difference in the regression slopes between the two groups (IPF-red, and donor-green).



**Figure 7**

ScRNA-seq analysis summary. A. Visualization of the different cell types in a uniform manifold approximation and projection (UMAP). B. UMAP representation of the cells from donor (eight samples) and IPF (eight sample) patients. C. The number of dysregulated TE subfamilies in eight fibrosis patients vs. eight donors in different cell types. A total of 77,517 single cells were profiled with scRNA sequencing. The analyses were performed using the Seurat (v3) R package. The cells were clustered using a graph-based shared nearest neighbor clustering approach, and 14 cell types were identified.

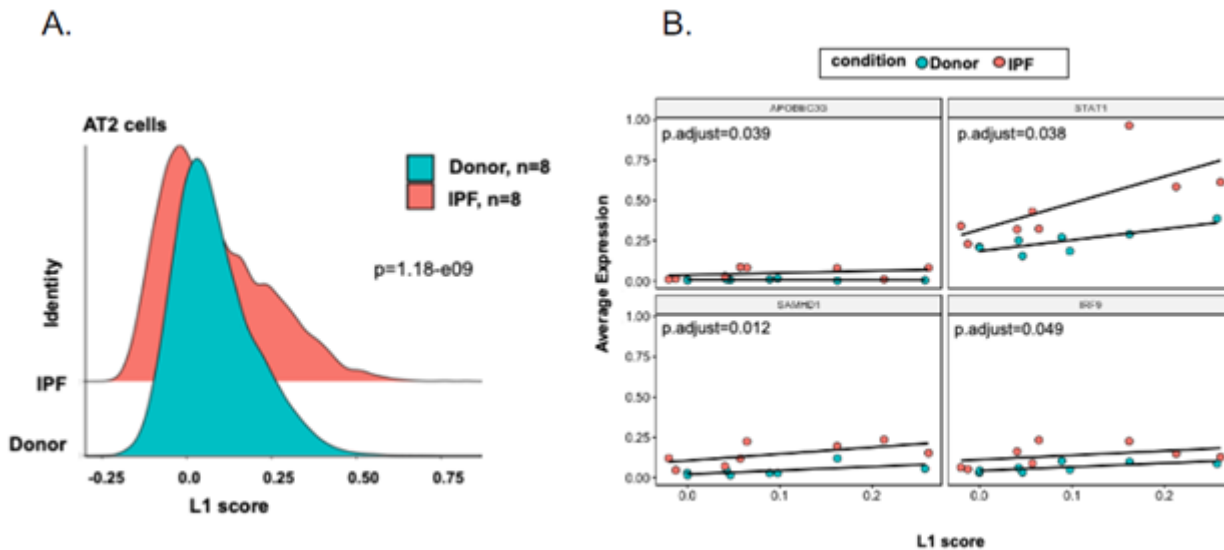


**Figure 8**

Differential L1 score distribution in the AT2 cells and its association with cellular factors. A. The L1 score differences in the AT2 cells from eight fibrotic (green) vs. eight normal (red) lungs ( $p = 1.18 \times 10^{-9}$ ,  $n = 8$  per phenotypic group). The L1 scores were calculated per each cell using all the expressed L1 elements, and the significance of the L1 score distribution between the phenotypes was determined using the Wilcoxon rank-sum test. The calculations were performed using the Seurat (v3) R package. B. Correlation plot showing the relationship between the TE L1 score and the individual TE-related cellular factors in the AT2 cells. The difference in the gene expression response to the L1 score in the AT2 cells was modeled using the `lm` function in R, the TE L1 score (independent variable), and the log<sub>2</sub>-transformed gene expression (dependent variable). To determine whether the relationship between L1 score and average gene expression differs between IPF and donors we used t-test. The p-value was corrected for multiple tests using the Benjamini and Hochberg (BH) test.

## Supplementary Files

This is a list of supplementary files associated with this preprint. Click to download.

- [FigS1.jpg](#)
- [FigS2.jpg](#)
- [FigS3.jpg](#)
- [SupplementalTable1.xlsx](#)
- [SupplementalTable2.xlsx](#)
- [SupplementalTable3.xlsx](#)
- [SupplementalTable4.xlsx](#)
- [SupplementalTable5.xlsx](#)

- [SupplementalTable6.xlsx](#)
- [SupplementalTable7.xls](#)